

Mission Planning for Multiple Autonomous Underwater Vehicles with Constrained In Situ Recharging

Priti Singh and Geoffrey A. Hollinger

Abstract—Persistent operation of Autonomous Underwater Vehicles (AUVs) without manual interruption for recharging saves time and total cost for offshore monitoring and data collection applications. In order to facilitate AUVs for long mission durations without ship support, they can be equipped with docking capabilities to recharge in situ at Wave Energy Converter (WEC) with dock recharging stations. However, the power generated at the recharging stations may be constrained depending on the sea conditions. Therefore, a robust mission planning framework is proposed using a centralized Evolutionary Algorithm (EA) and a decentralized Monte Carlo Tree Search (MCTS) method. Both methods incorporate the charge availability constraint at the recharging station in addition to the maximum charge capacity of each AUV. The planner utilizes a time-varying power profile of irregular waves incident at WECs for dock charging and generates efficient mission plans for AUVs by optimizing their time to visit the dock based on the imposed constraint. The effects of increasing the number of AUVs, increasing the number of points of interest in the mission area, and varying sea state on the mission duration are also analyzed.

I. INTRODUCTION

Multiple Autonomous Underwater Vehicles (AUVs) have the ability to navigate autonomously for prolonged periods in potentially hazardous environments by utilizing in situ recharging strategies. These environments are otherwise unsafe or time-consuming for human divers. Continuous operation of AUVs is essential for missions to carry out data collection, exploration, or monitoring in underwater environments. However, such AUVs typically require ship support, which is both costly and requires a trained human crew to be present during operation. Hence, AUV's can be equipped with docking capabilities that allow them to recharge at a docking station, and resume their mission without manual intervention.

Some missions allow tethered charging where AUVs are connected to an external power source using a tether cable. However, tethers can impose physical limitations on the maximum range covered by the AUV based on the cable length. On the other hand, docking stations can allow higher flexibility for AUV as these docking stations are often positioned at one or more fixed locations in the mission area allowing the AUVs to dock, recharge their batteries, and resume their mission. The power available at the docking station can be sourced from Wave Energy Converters (WECs). WECs capture energy from ocean waves and convert it

into electricity, which is then used to power the docking stations. The power generated at WECs is determined by the characteristics of the incident waves defined by the sea state as well as the design and efficiency of the converter [1]. Much of the existing work in generating efficient mission plans for AUVs fails to account for the energy constraint at the docking station, as it is assumed that the docks would always have surplus energy to completely recharge the AUVs [2]. In other scenarios that account for energy constraints at the dock, mission plans are executed such that AUVs visit the dock at periodic intervals and recharge completely [3]. The time between subsequent recharges ensures that the dock has sufficient power available. However, these assumptions come at the expense of higher mission time and energy consumption, as it might not be essential for an AUV to recharge completely or periodically. The sea state of a region can also exhibit significant variability seasonally due to various oceanographic factors [4]. The Water Power Technology Office's (WPTO) Wave Hindcast dataset provides an annual variation of the wave attributes for different regions [4].

Hence, efficient mission planning would ensure optimized utilization of vehicle energy resource as well as power generated by WECs. The power generated at the WECs varies based on the incidental wave conditions from calm sea state during summer to larger energetic waves during winter and early spring. Based on the specific mission goals and the power profile available at the docking stations, a mission planner can generate waypoints or routes for the AUV by efficiently minimizing energy consumption and travel time and at the same time maximizing mission coverage.

In this paper, a robust mission planning framework is designed for multiple AUVs that minimizes the mission duration while adhering to the energy constraints of both the AUVs as well as the docking station. The mission planning framework incorporating the energy constraints is provided using a centralized scheme based on Evolutionary Algorithm (EA) and a decentralized scheme based on Monte Carlo Tree Search (MCTS). The centralized EA approach generated mission plans with lesser mission time as compared to the decentralized MCTS approach at the cost of higher computational overhead. We obtained efficient mission plans on inclusion of time-varying power constraint at the docking station, as compared to AUVs assuming unlimited power at the docking station. This work is an extension of our previous workshop paper accepted in IROS 2nd Advanced Marine Robotics TC Workshop 2023.

The authors are with the Collaborative Robotics and Intelligent Systems Institute, Oregon State University, Corvallis, OR 97331, USA. {singhpri, geoff.hollinger}@oregonstate.edu

This work has been funded in part by NAVFAC contract N00024-21-D-6400/DO N0002421F8712.

II. RELATED WORK

A. AUV Docking and Recharging Systems

Underwater docking infrastructure provides a platform for AUV recharging and data transfer. The existing dock designs are classified as unidirectional and omnidirectional based on the direction in which AUV can approach the dock [5]. They are further categorized into fixed or floating type.

A WEC-dock hybrid system design allows on-site energy harvesting and AUV recharging capabilities [6]. A review of WEC technology is provided in [7] based on the location and type. The WEC device can be classified into oscillating water columns (OWCs), overtopping devices and oscillating bodies. Studies are also carried out to determine the optimal WEC size based on the incidental wave condition [8]. The type of docking mechanism decides the AUV navigation and undocking strategies.

B. Marine Energy Harvesting Model

Wave energy can be modelled using linear wave theory or models that take into account nonlinear waves effects and interactions. A simplified linear energy model for regular waves is a function of wave height H_m and wave period T_m as given by Equation 1, where ρ is the water density and g is the acceleration due to gravity [3]. Assuming a WEC-dock coupled system, the power generated at WEC can be computed using Equation 2, where B represents the WEC dimension, η is the hydrodynamic efficiency and ϵ_1 , ϵ_2 are generator efficiency and power transfer efficiency respectively:

$$J_{wave} = \frac{\rho g^2}{64\pi} T_m H_m^2 \quad (1)$$

$$P_{WEC} = J_{wave} B \eta \epsilon_1 \epsilon_2 \quad (2)$$

The wave spectral density function provides the significant wave height and energy period for irregular waves. The power matrix for a particular WEC type provides a mapping of the mean power available for a given sea state [9]. Sea states could vary seasonally due to wind patterns, tides, and currents creating calmer sea states in summer and larger energetic waves in winter.

Wave Energy Converter Simulator (WECSim) is an open source tool that incorporates complex wave energy modelling. The modelling involves numerical simulations or empirical relationships of wave steepness, water depth, wave spectra, and nonlinear wave interactions and generates power output based on the chosen WEC construction [10]. A time-varying power profile can be generated using WECSim by simulating the response of a specific WEC device to a given incident irregular wave condition.

Additionally, the power generated from WEC recharges the energy storage device at the dock such as batteries. The charging and discharging of the batteries can be modelled using the function as given in Equation 3, where β is the rate of charging and discharging:

$$\dot{q}(t) = \beta \quad (3)$$

C. Mission Planning Algorithms

Existing methods of mission planning for multiple autonomous vehicles mostly fall under the categories of centralized or decentralized approaches. In [11] and [12], a taxonomy for multirobot task allocation problems with inter-task dependencies is provided along with a mathematical formulation for each class of problems. A survey of collective behavior algorithms for multiagent systems provides a classification of the family of algorithms based on the underlying mathematical structure and provides insight into how the same algorithm can be applied to multiple applications [13].

A multi-objective genetic algorithm (GA) is utilized in [2] that generates energy efficient trajectories while accounting for obstacles and ocean currents. Such population based optimization approaches generate a candidate pool of possible solutions and iteratively improve upon them to converge to an approximate solution. In [14], Multi-Robot Long Term Persistent Coverage Problem (MRPCP) is formulated as Mixed Integer Linear Programming (MILP) that accounts for degree constraints, capacity and flow constraints, and fuel constraints. The method can also handle dynamic costs between the targets.

Multiagent reinforcement learning based methods for solving multiagent task allocation problems involves an MDP formulation that learns an optimal policy as the autonomous vehicles iteratively receive a reward for taking actions in the environment from their current state. A policy gradient based search is utilized to train all the robots independently, and is deployed in a decentralized manner where the robots are allowed to communicate about their completed tasks [15]. Other reinforcement learning approaches such as actor-critic based methods incorporate centralized learning and decentralized execution as those discussed in [16].

An online multiagent MCTS approach is applied in multi-drone delivery problem using dynamic coordination graphs [17]. The decentralized variant of MCTS is presented in [18] where every autonomous vehicle grows its own search tree and iteratively optimizes upon the action-sequence probabilities by communicating with other autonomous vehicles. In [19], an online distributed method for coordinating heterogeneous multirobot systems for task allocation is proposed. An optimal coverage problem under energy depletion and repletion constraints is developed using a hybrid system model that controls the switching between coverage and battery charging modes of all agents [20]. However, all the above methods assume unlimited power at the recharging stations, hence they do not account for power availability at the dock that can generate more informed mission plans for the autonomous vehicles.

III. METHODOLOGY

A. Problem Formulation

There are N AUVs that are assigned to cover all points of interest in the mission area at most once in minimum time. The mission area is represented as an undirected graph

$G = (V, E)$, where V represents the points of interest and recharging station nodes within the mission area such that $V_{dock} \subset V$, and E represents the edges connecting any two nodes in V . \mathcal{P} represents the set of AUV paths for all possible candidate solutions. $P_M = \{p_1, p_2, \dots, p_N\} \in \mathcal{P}$, where p_i represents the path of i^{th} AUV. $p_i = (v_1^i, v_2^i, \dots)$ is the sequence of nodes traversed by an i^{th} AUV, $v_j^i \in V$ represents the j^{th} point covered by i^{th} AUV. p_i determines when the i^{th} AUV would visit the recharging station. p'_i represents the set of nodes traversed by an i^{th} AUV. T_i represents the individual mission time of an i^{th} AUV.

Equation 5 defines that set V is equal to the total points of interest covered by all the AUVs. No overlapping constraint of points of interest covered by the i^{th} and j^{th} AUV in their respective mission plan p'_i , p'_j is given by Equation 6. The current charge $C_i(t)$ of the i^{th} AUV at any given time is bounded by its maximum charge capacity B_i as given in Equation 7. The charge available at the dock $q_{dock}(t)$ is bounded by its maximum charge capacity of B_{dock} as given in Equation 8. The current dynamic state of charge available at the dock is dependent on P_{WEC} (Equation 2), β (Equation 3), and $C_i(t)$ as given by a function f in Equation 9:

$$P_* = \operatorname{argmin}_{P_M \in \mathcal{P}} \max_{i=\{1,2,\dots,N\}} T_i \quad (4)$$

such that,

$$V = \bigcup_{i=\{1,2,\dots,N\}} p'_i \quad (5)$$

$$\forall_{i \neq j} \{p'_i \setminus V_{dock}\} \cap \{p'_j \setminus V_{dock}\} = \emptyset \quad (6)$$

$$0 \leq C_i(t) \leq B_i \quad (7)$$

$$0 \leq q_{dock}(t) \leq B_{dock} \quad (8)$$

$$q_{dock}(t) = f(C_{i=\{1,\dots,N\}}(t), P_{WEC}, \beta) \quad (9)$$

B. Algorithm

To solve the optimization problem formulated in Equation (4), a decentralized scheme using MCTS [21] as given in Algorithm 1 and a centralized scheme using an EA [22] [23] as given in Algorithm 2 is applied. The charge capacity of both AUVs and docking stations is incorporated into cost/fitness function implicitly as AUVs are penalized for a negative charge when they do not visit the docking station on time and rewarded otherwise. As the cost function provides a tradeoff between the total distance travelled and the total charge consumption for an entire mission, the visit to the docking station is an implicit function of the dock's current charge availability to meet the minimum incremental charge required by the AUVs for completing the mission.

In Algorithm 1, each i^{th} AUV builds its own tree until no mission point is unvisited. A node in the tree represents the point of interest in the mission area, AUV's state of charge, and possible next points of interest that can be traversed from the current point. Every AUV simultaneously takes one step in the environment through STEP 1-3 in lines 5-7, and updates its current state of charge using the *ChargeUpdate()* function in line 11. The AUV charge is updated based on the distance traveled from the current node

Algorithm 1 Decentralized mission planning framework using monte carlo tree search (MCTS) for multiple AUVs

- 1: **Input:** Graph G
- 2: **Output:** Mission time T_M , Path traced by each AUV p_i
- 3: **for** each episode **do**
- 4: Initialize $V_{unvisited} = V$, $root^i = \{v_{start}^i \forall i \in R\}$
- 5: **STEP 1** Perform selection for each AUV simultaneously until reaching a leaf node. Update the AUV charge and branch cost based on the distance traversed.
- 6: **STEP 2** Perform expansion in each AUV's tree and select a child for rollout if $V_{unvisited} \neq \emptyset$. Update the AUV charge and branch cost based on the selected child node.
- 7: **STEP 3** Perform simulation in each AUV's tree until $V_{unvisited} = \emptyset$.
- 8: **STEP 4** Backpropagate $\max_{i \in R} cost_i$ in each tree.
- 9: **STEP 5** Evaluate the policy and return the best sequence of points traversed by each AUV p_i if $V_{unvisited} = \emptyset$
- 10: **end for**

-
- 11: **Function:** *ChargeUpdate()*
 {▷Compute AUV/dock charge & branch cost}
 $c_{v_{next}}^i \leftarrow c_{v_{curr}}^i - c_i(v_{next}^i, v_{curr}^i)$
 - 12: **if** $v_{next}^i \in V_{dock}$ **then**
 - 13: $c_{dock} \leftarrow c_{dock} + \sum f(t)$
 - 14: $c_{v_{next}}^i \leftarrow c_{v_{next}}^i + \min\{c_{dock}, B_i - c_{v_{next}}^i\}$
 - 15: $c_{dock} \leftarrow \max\{0, c_{dock} - \min\{c_{dock}, B_i - c_{v_{next}}^i\}\}$
 - 16: **end if**
 - 17: $branch\ cost^i = -\frac{d(v_{next}, v_{curr})}{s_i} - \{c_{v_{curr}}^i - c_{v_{next}}^i\}$
-

Algorithm 2 Centralized mission planning framework using evolutionary algorithm for multiple AUVs

- 1: Initialize population P
 Each state in the population is represented as
 $p = \{v_{start}^1, v_1^1, v_2^1, \dots, v_{dock}^1;$
 $v_{start}^2, v_1^2, v_2^2, \dots, v_{dock}^2; \dots\}$ where, $v \in V$
 - 2: **for** each episode **do**
 - 3: **STEP 1** Evaluate Fitness F :
 {▷Update dock & i^{th} AUV's current charge}
 $c_{v_{next}}^i \leftarrow c_{v_{curr}}^i - c_i(v_{next}^i, v_{curr}^i)$
 $c_{dock} \leftarrow c_{dock} + \sum f(t)$
 $F \leftarrow F + c_{v_{next}}^i$
 - 4: **if** ($v_{next}^i \in V_{dock}$ & $c_{dock} > 0$) **then**
 - 5: $\Delta c^i = \max\{c_{dock}, B_i - c_{v_{next}}^i\}$
 - 6: $F \leftarrow F + \Delta c^i$
 - 7: **else if** $c_{dock} = 0$ **then**
 - 8: $F \leftarrow F - B_{dock}$ {▷Add penalty}
 - 9: **end if**
 - 10: **STEP 2** Perform Roulette Selection and save k candidates for next generation.
 - 11: **STEP 3** In the remaining $P - k$ candidates, perform mutation by selecting a state from each robot path such that the current state $\notin \{v_{start}, v_{dock}\}$
 - 12: **end for**
-

to the next node. If the destination is a docking location (line 12), the AUV is recharged based on the current charge available at the docking station. In STEP 4, the cost of the terminal state for each AUV is computed as given in line 17 and the cost is backpropagated from the starting node in the simulation phase to the root node.

In Algorithm 2, a population of possible solutions P is randomly generated. Each state p is encoded such that each AUV's path has nodes corresponding to starting node, docking node and a random sequence of mission points of interest. All AUVs start from the same point v_{start}^i . The docking node v_{dock}^i in each AUV's path is non-interchangeable during mutation with any other AUV's path. All other mission points of interest are interchangeable across the entire possible solution during mutation. In STEP 1 (lines 3-9), the fitness of each member solution in the population is evaluated using a cost function that penalizes cost of traveling between two points and an added penalty for reaching the docking station when the dock has no charge left. Any incremental change in AUV's charge at the dock Δc^i is added as a reward to the cost function. A fraction of solutions from the population are selected based on Roulette selection [24] for continuing in the next generation. The remainder of the next generation of population is formed by mutating the selected candidates from the roulette selection. The process is repeated until the fitness value converges.

The converged policy using both algorithms provides the sequence of nodes traversed by each AUV, which also dictates when the AUV would visit the dock through the course of a mission.

IV. SIMULATION & RESULTS

A. Simulation Setup

The above algorithms are evaluated using maps with a random distribution of nodes in a $60 \text{ km} \times 60 \text{ km}$ area. The dock is represented by one of the points on the map. The dock is assumed to have a maximum charge capacity lesser than or equivalent to a single AUV and can only charge one AUV at a time in all the simulations following Sec. IV-B. The assumed AUV battery capacity allows it to travel continuously for 15 hr before recharging. The recharge time is assumed to be negligible with respect to the total uninterrupted travel time of the AUV. Mission duration by increasing the number of AUVs, increasing the number of points of interest in the same mission area, and in different sea state conditions using constant mean power or time-varying power profile for dock charging.

In our experiments, it is assumed that all the AUVs would start from the same starting location and would need to recharge once or twice at the docking stations to complete the entire mission in the least amount of time. Moreover, the proposed framework can be extended for multiple docks or for multiple recharges at the same docking station. The dock charges linearly based on either a constant mean power or non-linearly using a time-varying power profile. A low and high sea state representing seasonal variation is considered to understand the impact on the total mission duration. The

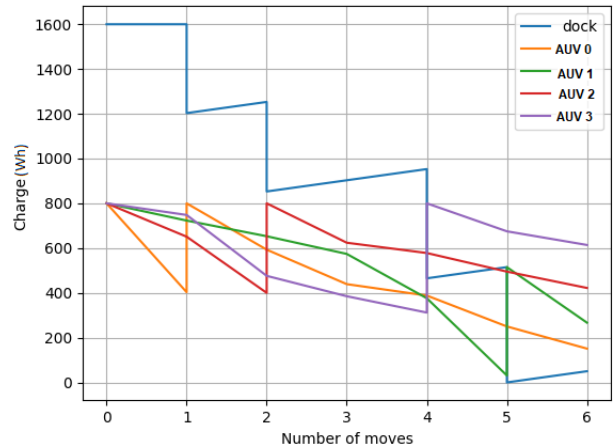


Fig. 1. Charging and discharging profile for four AUVs $\{0, 1, 2, 3\}$ and the *dock* node through the course of mission in a $60 \text{ km} \times 60 \text{ km}$ area with 18 randomly distributed points of interest. Number of moves along y-axis represents charge used while moving from one mission interest point to another.

TABLE I
COMPUTATION TIME OF ALGORITHM 1 (MCTS), AND ALGORITHM 2 (EA) FOR A SINGLE ITERATION.

Computation Time (secs)				
Number of nodes	10	14	18	22
EA	11.83	13.26	14.82	16.10
MCTS	2.42	4.32	7.638	11.41
Number of agents	2	4	6	8
EA	17.55	18.52	20.24	22.56
MCTS	22.03	14.97	13.5	12.38

AUV discharges linearly with distance traveled as shown in Fig. 1 [25]. Experiments are also carried out using a time-varying power profile for an irregular incident wave condition.

The methods described in Section III-B were implemented using Python 3.9.7, and the simulations were carried out on a Dell Inspiron 7501 with Intel(R) Core(TM) i7-10750H CPU@2.6GHz, 6 Core(s), and NVIDIA(R) GeForce GTX(R) 1650 Ti.

B. Results & Analysis

1) *Using constant mean power for dock charging:* The total mission time is evaluated against an increasing number of AUVs as well as an increasing number of mission points of interest using both algorithms as shown in Fig. 2. The computed mission time was also analysed for a low and high sea state scenario as shown in Fig. 3. In the high sea state scenario, the WEC is assumed to generate double the power than the power generated in the low sea state scenario.

It is observed that Algorithm 2 (EA) generates plans with reduced mission time for the constrained energy source problem than Algorithm 1 (MCTS). However, the centralized EA scheme has a higher computational overhead than the decentralized MCTS scheme as it requires one central planner that generates the sequence of mission points of interest to be traversed by each AUV in the entire fleet. Table I represents the computational complexity of both algorithms for a single

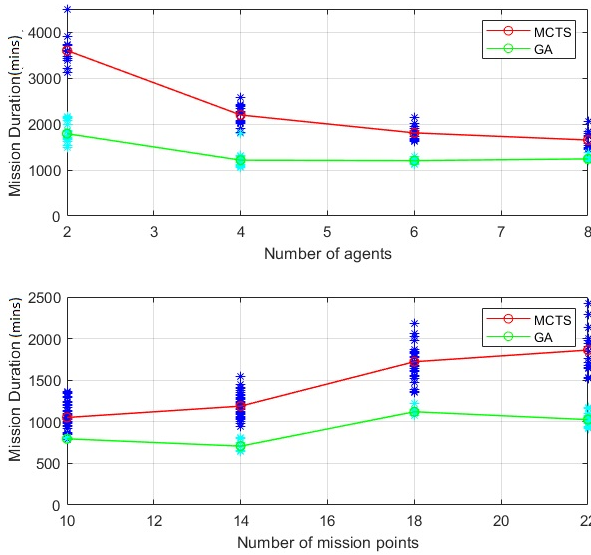


Fig. 2. (Top) Mission duration with an increasing number of AUVs with 26 randomly distributed nodes, and (Bottom) increasing number of nodes in a $60 \text{ km} \times 60 \text{ km}$ mission area with two AUVs. The centralized EA framework generates mission plans with lower durations than the decentralized MCTS framework for the constrained energy source problem.

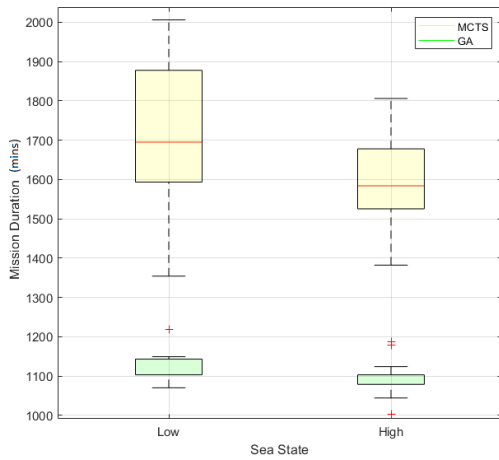


Fig. 3. Mission duration for a low and high sea state condition with four AUVs and one dock in a $60 \text{ km} \times 60 \text{ km}$ area with 18 randomly distributed points of interest. In this mission scenario, higher sea state generates more efficient mission plans that at low sea state and the impact can be seen from reduced mission time.

iteration under the same simulation conditions as in Fig. 2. On comparing the mission duration in low and high sea state scenarios as shown in Fig. 3, it is observed that the mean value of mission duration obtained over multiple episodes decreases for a high sea state condition. The observation indicates that the AUVs were able to optimize their visit time to the recharging station more efficiently in the high sea state condition since the maximum power availability constraint at the dock is relaxed as compared to the low sea state condition.

2) Using time-varying power profile for dock charging:

The mission planning framework is extended to include a time-varying power profile for the charging stations as discussed in [26]. The time-varying power profile captures the irregular wave condition that relates more closely to an actual

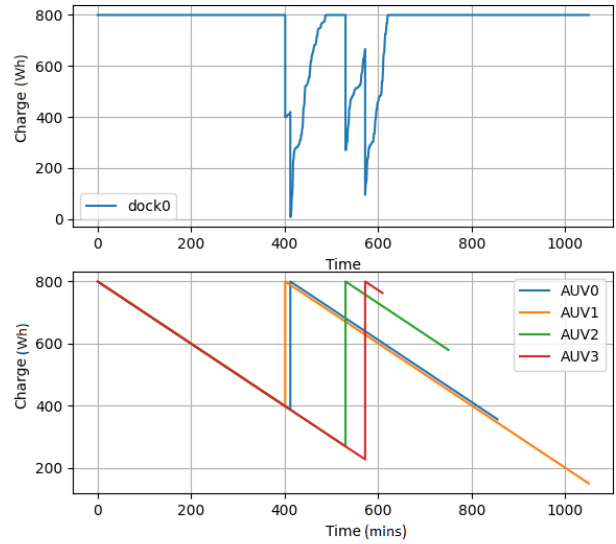


Fig. 4. Charge consumption using four AUVs, one dock with 18 points of interest on a $60 \text{ km} \times 60 \text{ km}$ mission area. Dock charges using a time-varying power profile for an irregular wave condition.

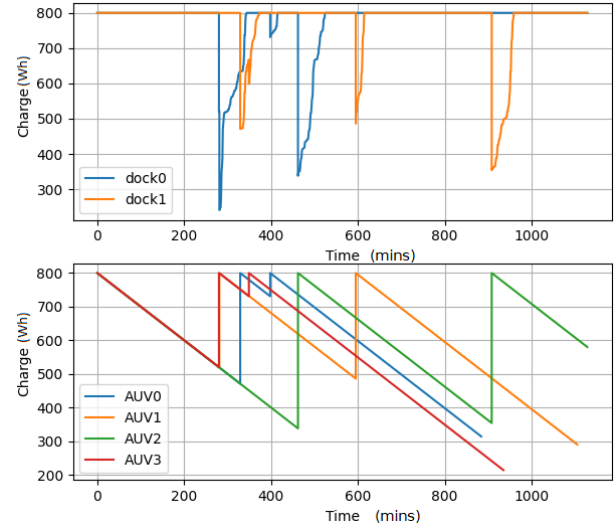


Fig. 5. Charge consumption using four AUVs, two docks with 27 points of interest on a $60 \text{ km} \times 60 \text{ km}$ area. Dock charges using a time varying power profile for an irregular wave condition.

condition at sea as compared to the linear charging profile as shown in Fig. 1. Two simulation scenarios are considered that include four AUVs, one dock with 18 mission points of interest, and four AUVs, two docks with 27 mission points of interest. In Fig. 4 and Fig. 5, the top figure represents the non-linear charging behaviour of the dock using the power profile. Fig. 5 shows the scalability of the mission planning framework to multiple docks with higher number of mission points of interest. For incorporating a given time-varying power profile, the dock charge is obtained by integrating power at every time step such that the integration time step would be less than the time step at which power data is sampled in the given profile. Hence, this provision allows efficient mission planning for different sea conditions with any complex time-varying power profile.

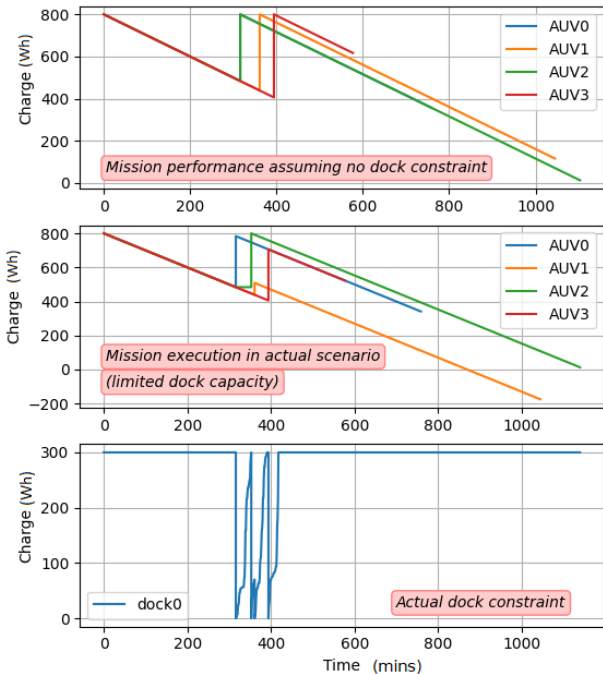


Fig. 6. Mission scenario consisting of four AUVs, one dock, and 18 randomly generated points of interest on a $60 \text{ km} \times 60 \text{ km}$ mission area. (Top) Expected charge profile of all AUVs for a mission plan that was generated assuming unlimited power at the dock. (Middle) Actual charge profile of all AUVs when the mission plan was executed in an environment with limited charge capacity of the dock. (Bottom) Actual charge variation of the dock.

The impact of incorporating the dock's charge capacity constraint within the mission planning framework was analyzed by comparing the mission performance without accounting for this constraint. Without the dock charge constraint, AUVs would assume unlimited charge availability at the docks during their visit to the docking station. Fig. 6 represents one such scenario where the mission plans were generated without the dock charge constraint. However, the mission performance degraded when the AUVs executed these plans in the actual scenario with limited charge capacity at the dock.

Fig. 6-(Top) represents the expected charge profile for all the AUVs generated using Algorithm 2 assuming unlimited charge availability at the docking station. However, when AUVs executed their respective mission plans in the actual environment where the charge available at the dock was limited, the total mission time increased by 37 mins along with AUV1 shutting down before completing its intended mission plan as seen in Fig. 6-(Middle). The increase in mission time is because AUV2 has to wait for the dock to recharge since AUV0 discharges the dock completely. Moreover, AUV1 is unable to charge completely since the current charge available at the dock in the actual environment is not sufficient for AUV1 to complete its mission. Fig. 6-(Bottom) represents the actual charge availability at the docking station.

Hence, mission plans can be improved by incorporating

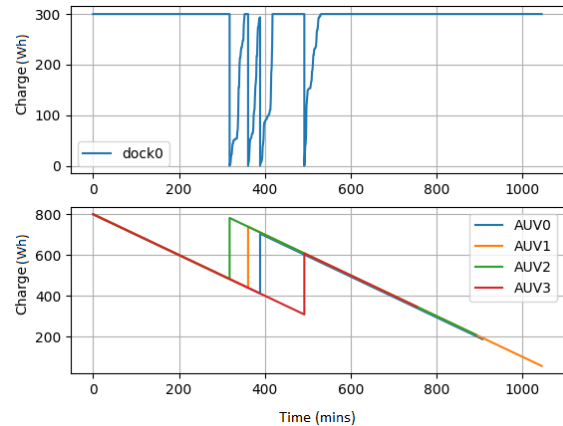


Fig. 7. Mission scenario consisting of four AUVs, one dock and 18 randomly generated points of interest on a $60 \text{ km} \times 60 \text{ km}$ area. (Bottom) Charge profile of AUVs for the mission plan generated with the incorporation of the dock limited charge capacity constraint. (Top) The dock's current state of charge is determined using a time-varying power profile.

the charging constraint at the docking station. Fig. 7 represents the improved mission plans generated with Algorithm 2 incorporating the actual charge available at the dock. The current charge at the dock is computed by integrating the time-varying power profile. Using the improved plans, the AUVs were able to complete the mission with non-negative remaining charge and with lesser mission time as compared to the previous scenario in Fig. 6.

V. CONCLUSIONS

A centralized framework using an EA and a decentralized framework using MCTS are provided for the mission planning of multiple underwater vehicles that take into account the charge available at the recharging station in addition to the charge capacity of AUVs. The impact of an increasing number of AUVs and an increasing number of points of interest on the overall mission duration was compared against the two algorithms. The mission performance was analyzed with respect to changing sea state conditions. Improved mission plans were obtained through incorporation of the charge capacity constraint of the docking station as compared to mission plans that assume unlimited power at the docking station.

In the future, mission performance can be studied by incorporating charging time delays at the recharging station. Additionally, the continuous communication dependency of a central planner during online replanning can be overcome with a decentralized scheme. Hence, the mission performance can be analyzed for online replanning scenarios as well as AUV failure scenarios.

ACKNOWLEDGMENT

I am deeply appreciative of Ian C. Rankin's willingness to engage in insightful discussions, share his expertise, and offer constructive feedback throughout the entire research process.

REFERENCES

- [1] R. Waters, "Energy from ocean waves: full scale experimental verification of a wave energy converter," Ph.D. dissertation, Universitetsbiblioteket, 2008.
- [2] B. Li, B. Moridian, A. Kamal, S. Patankar, and N. Mahmoudian, "Multi-robot mission planning with static energy replenishment," *Journal of Intelligent & Robotic Systems*, vol. 95, pp. 745–759, 2019.
- [3] B. P. Driscoll, L. A. Gish, and R. G. Coe, "A scoping study to determine the location-specific wec threshold size for wave-powered auv recharging," *IEEE Journal of Oceanic Engineering*, vol. 46, no. 1, pp. 1–10, 2020.
- [4] W.-C. Wu, T. Wang, Z. Yang, and G. García-Medina, "Development and validation of a high-resolution regional wave hindcast model for us west coast wave resource characterization," *Renewable Energy*, vol. 152, pp. 736–753, 2020.
- [5] A. M. Yazdani, K. Sammut, O. Yakimenko, and A. Lammas, "A survey of underwater docking guidance systems," *Robotics and Autonomous systems*, vol. 124, p. 103382, 2020.
- [6] J. Wallen, N. Ulm, and Z. Song, "Underwater docking system for a wave energy converter based mobile station," in *Proc. IEEE/MTS OCEANS Conference, Seattle*, 2019.
- [7] B. Drew, A. R. Plummer, and M. N. Sahinkaya, "A review of wave energy converter technology," 2009.
- [8] B. Robertson, G. Dunkle, T. Mundon, and L. Kilcher, "Wave resource spatial and temporal variability dependence on wec size," *International Marine Energy Journal*, vol. 5, no. 1, pp. 113–121, 2022.
- [9] [Online]. Available: <https://apps.openei.org/swec/>
- [10] K. Ruehl, D. Ogden, Y.-H. Yu, A. Keester, N. Tom, D. Forbush, J. Leon, J. Grasberger, and S. Husain, "Wec-sim v5.0.1," 2022. [Online]. Available: <https://zenodo.org/badge/latestdoi/20451353>
- [11] G. A. Korsah, A. Stentz, and M. B. Dias, "A comprehensive taxonomy for multi-robot task allocation," *The International Journal of Robotics Research*, vol. 32, no. 12, pp. 1495–1512, 2013.
- [12] G. Dudek, M. R. Jenkin, E. Milios, and D. Wilkes, "A taxonomy for multi-agent robotics," *Autonomous Robots*, vol. 3, pp. 375–397, 1996.
- [13] F. Rossi, S. Bandyopadhyay, M. T. Wolf, and M. Pavone, "Multi-agent algorithms for collective behavior: A structural and application-focused atlas," *arXiv preprint arXiv:2103.11067*, 2021.
- [14] D. Mitchell, M. Corah, N. Chakraborty, K. Sycara, and N. Michael, "Multi-robot long-term persistent coverage with fuel constrained robots," in *Proc. IEEE international conference on robotics and automation (ICRA)*, 2015, pp. 1093–1099.
- [15] S. Manjanna, M. A. Hsieh, and G. Dudek, "Scalable multirobot planning for informed spatial sampling," *Autonomous Robots*, vol. 46, no. 7, pp. 817–829, 2022.
- [16] G. Bono, J. S. Dibangoye, L. Matignon, F. Pereyron, and O. Simonin, "Cooperative multi-agent policy gradient," in *Machine Learning and Knowledge Discovery in Databases*. Springer, 2019, pp. 459–476.
- [17] S. Choudhury, J. K. Gupta, P. Morales, and M. J. Kochenderfer, "Scalable anytime planning for multi-agent mdps," in *Proc. of the 20th International Conference on Autonomous Agents and MultiAgent Systems*, 2021, pp. 341–349.
- [18] G. Best, O. M. Cliff, T. Patten, R. R. Mettu, and R. Fitch, "Decmets: Decentralized planning for multi-robot active perception," *The International Journal of Robotics Research*, vol. 38, no. 2-3, pp. 316–337, 2019.
- [19] A. J. Smith, G. Best, J. Yu, and G. A. Hollinger, "Real-time distributed non-myopic task selection for heterogeneous robotic teams," *Autonomous Robots*, vol. 43, pp. 789–811, 2019.
- [20] X. Meng, A. Houshmand, and C. G. Cassandras, "Multi-agent coverage control with energy depletion and repletion," in *IEEE Conference on Decision and Control (CDC)*, 2018, pp. 2101–2106.
- [21] C. B. Browne, E. Powley, D. Whitehouse, S. M. Lucas, P. I. Cowling, P. Rohlfshagen, S. Tavener, D. Perez, S. Samothrakis, and S. Colton, "A survey of monte carlo tree search methods," *IEEE Transactions on Computational Intelligence and AI in games*, vol. 4, no. 1, pp. 1–43, 2012.
- [22] T. Bäck and H.-P. Schwefel, "An overview of evolutionary algorithms for parameter optimization," *Evolutionary computation*, vol. 1, no. 1, pp. 1–23, 1993.
- [23] D. Whitley, "A genetic algorithm tutorial," *Statistics and computing*, vol. 4, pp. 65–85, 1994.
- [24] K. Jebari, M. Madiafi *et al.*, "Selection methods for genetic algorithms," *International Journal of Emerging Sciences*, vol. 3, no. 4, pp. 333–344, 2013.
- [25] J. Bi, Y. Wang, and J. Zhang, "A data-based model for driving distance estimation of battery electric logistics vehicles," *EURASIP Journal on Wireless Communications and Networking*, vol. 2018, no. 1, pp. 1–13, 2018.
- [26] M. Chen, R. Vivekanandan, C. J. Rusch, D. Okushemiya, D. Manalang, B. Robertson, and G. A. Hollinger, "A unified simulation framework for wave energy powered underwater vehicle docking and charging," *Applied Energy*, vol. 361, p. 122877, 2024.